Article

Evaluation of Flow Resistance Models Based on Field Experiments in a Partly Vegetated Reclamation Channel

Giuseppe Francesco Cesare Lama [1,*], **Alessandro Errico** [2], **Simona Francalanci** [3], **Luca Solari** [3], **Federico Preti** [2] and **Giovanni Battista Chirico** [1]

[1] Department of Agricultural Sciences, Water Resources Management and Biosystems Engineering Division, University of Naples Federico II, 80055 Portici (NA), Italy; giovannibattista.chirico@unina.it
[2] Department of Agricultural, Food, Environmental and Forestry Sciences and Technologies, University of Florence, 50144 Firenze, Italy; alessandro.errico@unifi.it (A.E.); federico.preti@unifi.it (F.P.)
[3] Department of Civil and Environmental Engineering, University of Florence, 50139 Firenze, Italy; simona.francalanci@unifi.it (S.F.); luca.solari@unifi.it (L.S.)
* Correspondence: giuseppefrancescocesare.lama@unina.it; Tel.: +39-081-253-9423

check for updates

Abstract: This study presents a methodology for improving the efficiency of Baptist and Stone and Shen models in predicting the global water flow resistance of a reclamation channel partly vegetated by rigid and emergent riparian plants. The results of the two resistance models are compared with the measurements collected during an experimental campaign conducted in a reclamation channel colonized by Common reed (*Phragmites australis (Cav.) Trin. ex Steud.*). Experimental vegetative Chézy's flow resistance coefficients have been retrieved from the analysis of instantaneous flow velocity measurements, acquired by means of a downlooking 3-component acoustic Doppler velocimeter (ADV) located at the channel upstream cross section, and by water level measurements obtained through four piezometers distributed along the reclamation channel. The main morphometrical vegetation features (i.e., stem diameters and heights, and bed surface density) have been measured at six cross sections of the vegetated reclamation channel. Following the theoretical assumptions of the divided channel method (DCM), three sub-sections have been delineated in the reference cross section to represent the impact of the partial vegetation cover on the cross sectional variability of the flow field, as observed with the ADV measurements. The global vegetative Chézy's flow resistance coefficients have been then computed by combining each resistance model with four different composite cross section methods, respectively suggested by Colebatch, Horton, Pavlovskii, and Yen. The comparative analysis between the modeled and the experimental vegetative Chézy's coefficients has been performed by computing the relative prediction error (ε_r, expressed in %) under two flow rate regimes. Stone and Shen model combined with the Horton composite cross section method provides vegetative Chézy's coefficients with the lowest ε_r.

Keywords: partly vegetated reclamation channel; Common reed; resistance models; vegetative Chézy's coefficient; DCM; composite cross section

1. Introduction

The presence of backwater in manmade reclamation channels enhances the growth of riparian vegetation, promoting the expansion of aquatic and terrestrial habitats and improving water quality [1,2]. In this context, the analysis of the real-scale interaction between riparian plants and water flow in vegetated channels can provide relevant hints to the administrators of land reclamation areas, about

the most useful approaches to be followed when managing the riparian vegetation, which can ensure the conveyance capacity of the channel with limited impacts on the natural habitats [1].

One of the most challenging tasks when programming the management of riparian vegetation in reclamation channels is the definition of simple and accurate models for assessing the global flow resistance coefficients (e.g., the vegetative Chèzy flow resistance coefficient C_r [3,4], the Manning's n hydraulic roughness coefficient [5], the vegetative Darcy-Weisbach's friction factor f'' [6]). However, the predictive efficiencies of these models have been rarely evaluated with field experimental data, especially in partly vegetated channels [1,5]. In their study, the authors analyzed the effect of a condition of partial riparian vegetation on flow dynamics and turbulence features related to the presence of both rigid [1] and flexible [5] invasive riparian vegetation.

The global flow resistance generated in vegetated channels could be estimated by employing many models, also known as "resistance predictors" [4]. Each model has been derived under distinct hydraulic (laboratory flumes or real vegetated channels) and vegetative (real or artificial riparian plants) conditions [1,6,7]. Among others, the Baptist et al. [8] and the Stone and Shen [9] resistance models (hereinafter referred to as Bp and S&S [8,9]) have been validated for real riparian vegetation, considering both emergent and submerged vegetative conditions, depending on the ratio between the water level (h) and the plants height above the vegetated channel bottom (h_v).

The present study aims at evaluating the efficiency of Bp and S&S resistance models [8,9] by exploiting experimental data retrieved from field hydrodynamic and vegetative measurements, realized by Errico et al. [1] within an abandoned vegetated reclamation channel located in northern Tuscany (Italy). The main species observed along the entire reclamation channel was the Common reed, a riparian species widespread in lowlands and wetlands [10]. The examined emergent riparian reed plants were at a dormant phenological stage, characterized by rigid stems. A first comparison between modeled and measured C_r has been executed without considering the variability of the cross-sectional flow velocity field induced by the partial vegetation cover. Thus, Bp and S&S resistance models [8,9] have been applied under the assumption that the entire cross section homogenously contributes to the global flow resistance process. A second comparative analysis has been realized by applying a methodology based on the combination of the well-known divided channel method (DCM) [11] with four composite cross section methods, as respectively proposed by Colebatch [12], Horton [13], Pavlovskii [14], and Yen [15]. DCM has been applied to represent the impact of the non-homogenous distribution of the riparian reed along the wetted perimeter by dividing the entire cross section into three sub-sections: orographic left side, central region, and orographic right side. All comparative analyses have been carried out with two different flow rates, under stationary flow conditions.

The outcomes of this study could constitute a suitable tool for future research in ecohydraulics, especially for the computation of the real-scale effect of partial riparian vegetation cover on global flow resistance in natural and artificial water bodies.
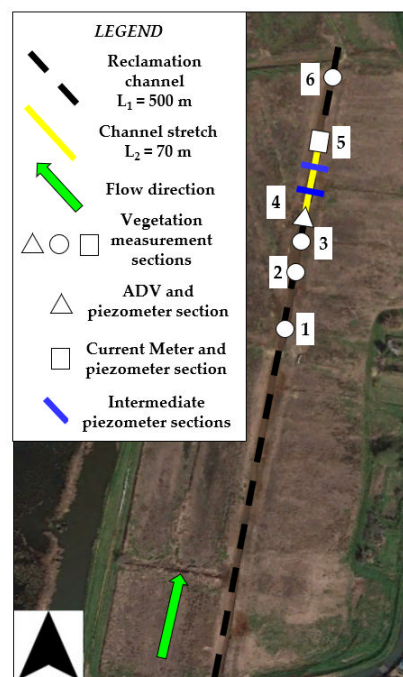
2. Materials and Methods

2.1. Experimental Area

The vegetative and hydrodynamic (streamwise velocities and water levels) field measurements were conducted in an abandoned vegetated reclamation channel, which drained field plots that had not been cultivated in the previous 5 years [1,10]. As depicted in Figure 1, the vegetated reclamation channel belongs to a lowland in hydraulic connection with the Massaciuccoli Lake, located in northern Tuscany (Italy).

The 500-m long vegetated reclamation channel was covered by emergent Common reed, at a dormant phenological stage [1]. Field hydrodynamic and vegetation measurements were taken at six cross sections of the vegetated reclamation channel (Figure 2).

Figure 1. Location of the experimental area (indicated by the yellow filled circle), in hydraulic connection with the adjacent Massaciucoli Lake (indicated by the red filled circle). (From https://www.esa.int/ESA_Multimedia/Images/2010/07/La_Toscana_vista_da_Envisat, modified).

Figure 2. Surveyed cross sections (1–6) along the 500-m long vegetated reclamation channel, indicated by the black dashed line. The 70-m long experimental channel stretch is indicated by the yellow continuous line. The white filled circles indicate the measuring sections employed for the measurements of the vegetative morphometrical properties, while the white filled triangle and square represent the ADV and current meter measuring cross section, which coincides with the upstream cross section of the 70 m long experimental channel stretch, also employed for the water tables measurements. The blue continues lines indicate the other two intermediate water level measuring cross sections. (From Lama et al. [3], modified).

The distances between pairs of adjacent cross sections were the following:

- *Cross sections 1–2*: 39 m;
- *Cross sections 2–3*: 28 m;

- 　　　*Cross sections 3–4*: 27 m;
- 　　　*Cross sections 4–5*: 70 m;
- 　　　*Cross sections 5–6*: 35 m.

The field hydrodynamic and vegetation measurements were designed to characterize the hydraulic properties (cross sectional flow velocity fields and hydraulic gradient), and the reed plant density and morphometrical properties (diameter and height from the channel bottom). As indicated by Errico et al. [1], to reduce the uncertainties during the field hydrodynamic measurements, the hydrodynamic analyses were restricted to a 70-m long experimental stretch of the 500-m long channel, since in this stretch the cross sections were almost uniform in shape. The vegetational measurements were taken along only half of the 500-m long channel because the other half was not easily accessible, because of the presence of gas pipes, hydraulic crossings, and small bridges.

2.2. Field Hydrodynamic Experiments

The field hydrodynamic experiments inside the 70-m long experimental channel stretch were carried out with six different flow rates. In this study, we examine just the two flow rates that were established under the condition of partial riparian vegetation cover. Following Errico et al. [1], hereinafter these two flow rates are respectively referred to as $Q_2 = 0.16$ m^3·s^{-1} and $Q_3 = 0.33$ m^3·s^{-1}. The other flow rates not examined in this study are: one with full vegetation coverage, equal to 0.126 m^3·s^{-1}; three with no vegetation coverage, respectively equal to 0.086 m^3·s^{-1}, 0.175 m^3·s^{-1}, and 0.277 m^3·s^{-1}.

Because of time constraints and limited available resources for the field campaign, we have not been able to explore a larger number of flow rates and water levels.

The flow rates were established by four mobile hydro-pumps, regulated by the engines of four agricultural tractors: two hydro-pumps were discharging into the entire reclamation channel, at the upstream end, by pumping the water from the adjacent Massaciuccoli Lake; the other two were pumping at the same flow rate out of the channel, at downstream end. The pumping regimes at the beginning and the end of the 500-m long vegetated reclamation channel have been simultaneously regulated to establish stationary conditions during the field hydrodynamic experiments. Stationary flow has been assumed to be verified when the water levels measured at the stages of four cross sections (Section 4, Section 5 and two intermediate cross sections located at a mutual distance of approximately 23 m apart) were verified to be stable for a time interval of 30 min. Flow rate Q_2 corresponds to the minimum flow rate achievable with the pumping system deployed in the field, while flow rate Q_3 corresponds to the channel flow at bankfull stage.

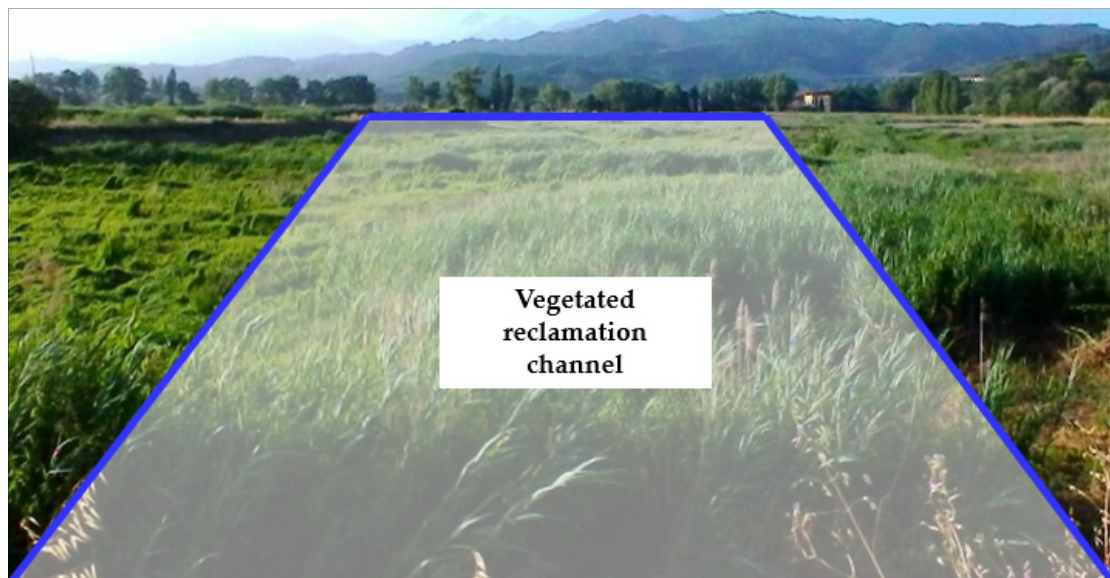### 2.3. Measurements of the Morphometrical Vegetation Properties

Morphometrical properties of the examined riparian vegetation (stem diameters, plant's heights and density, defined as the number of plants for unit bed surface area) have been measured along the wetted perimeters of the six selected cross sections of the reclamation channel (Figure 3).

Details about the riparian vegetation field survey activity can be found in the study by Errico et al. [1].
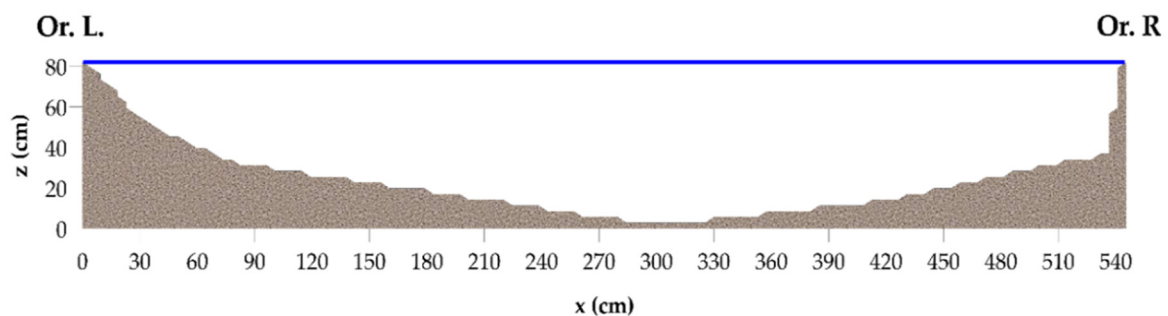
The measured field morphometrical vegetation properties have been afterward employed as input parameters of the two resistance predictor models examined in the present study.

2.4. Measurements of the Hydrodynamic Characteristics

The upstream cross section of the experimental reclamation channel stretch (indicated as Section 4 in Figure 2) was selected for the flow velocity measurements (mean flow velocity and turbulence fluctuations [16,17]). A 3-component Nortek$^\circledR$ acoustic Doppler velocimeter (ADV) Vectrino II device has been employed, equipped with a 4-beam down-looking probe. The ADV cross section is illustrated in Figure 4.

Figure 3. View of the 500-m long vegetated reclamation channel. The continuous blue lines indicate the borders of the vegetated reclamation channel.
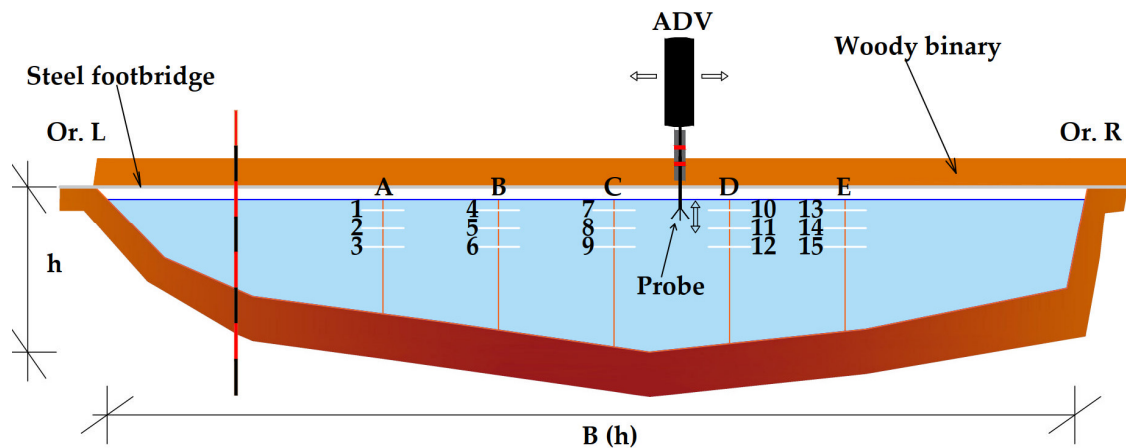

Figure 4. Acoustic Doppler velocimeter (ADV) cross section. The continuous dark blue line indicates the water level at bankfull.

Many studies dealing with the interaction between water flow and riparian vegetation have been conducted by employing ADV devices, especially in laboratory flumes [17,18], but just in few cases it has been employed in real manmade channels covered by living riparian vegetation [1,5]. An OTT® C31 propeller-type universal current meter has been located at the downstream cross section of the experimental reclamation channel stretch (indicated as Section 5 in Figure 2) to monitor the water flow velocity aiming at verifying the continuity of the water flow volume in the experimental channel stretch [1].

As indicated in Figure 2, the *ADV* local flow velocity measurements have been taken at 15 points, uniformly distributed along five hydrometric vertical lines spaced 65-cm apart (Figure 5). Three measuring points have been investigated at each hydrometric line, corresponding respectively to depths of 0.05, 0.17, and 0.27 m below the water surface. The *ADV* measurement depths from the water surface have been maintained fixed, regardless of the water level registered under each examined flow rates in the vegetated reclamation channel.

The ADV raw data are represented by continuous signals over time. Then, in order to improve the quality of the local flow velocity measurements [1], they have been pre-processed [19,20] to remove the noise from the acquired signals. As reported in Errico et al. [1], the values of the signal to noise ratio (SNR, expressed in dB) referred to the two flow rates examined in this study were equal to 38.05 dB and 55.77 dB for Q_2 and Q_3 flow rates, respectively. Both SNR values are higher than the minimum threshold value reported by Goring and Nikora [20], which is equal to 15 dB.

Figure 5. Scheme of the ADV measuring points (1–15), uniformly distributed along five hydrometric lines (A–E). The ADV moved along a woody binary installed on a steel footbridge, and then blocked at each measuring point during the acquisitions. The two parameters h (m) and B (m) are respectively the water level and width at bankfull of the ADV cross section, which vary according to the flow rate. The continuous dark blue line indicates the water level at bankfull. (from Errico et al. [1], modified).

The hydraulic gradient has been calculated as the slope of the water surface, retrieved from the water level measurements realized at four piezometers distributed along the experimental channel stretch [1,21], as indicated in Figure 2.

2.5. Partial Riparian Vegetation Coverage

The condition of partial riparian vegetation coverage has been obtained by mechanically removing all stems falling inside a 2.70 m wide central region of the entire reclamation channel [1], by means of machinery employed in riparian Common reed management activities [22,23], leaving two side buffers of undisturbed riparian vegetation (Figure 6a). Previous studies have highlighted that with this type of vegetation management strategy it is possible to mitigate the disturbance of the riparian habitat while increasing the channel conveyance to values comparable with that obtained by totally clearing the riparian vegetation [1,5,24]. In the case of partial riparian vegetation coverage, the flow velocity measurements have been conducted by sliding the ADV device along the entire wetted perimeter, in order to characterize the flow fields in correspondence of both the clear and the vegetated regions of the measuring cross section, and, most importantly, at their physical interface, as indicated in Figure 6b.

Figure 6. (**a**) Examined vegetated reclamation channel in condition of partial riparian vegetation coverage; (**b**) local *ADV* flow velocity measurement set-up, for the two investigated flow rate regimes $Q_2 = 0.16$ m^3·s^{-1} and $Q_3 = 0.33$ m^3·s^{-1}.

During the field hydrodynamic experiments, we observed the presence of dead leaves, stems, and rhizomes at the reclamation channel bottom, concentrated in a 10–15 cm thick layer, because of the

mechanical action of the cutting machinery. This residual vegetative material importantly affected the cross sectional velocity distributions and, hence, the experimental global flow resistance, as illustrated in the study by Errico et al. [1].

2.6. Measured Vegetative Chézy's Flow Resistance Coefficients: $C_{r, meas}$

Under the assumptions of uniform flow established in the reclamation channel characterized by a condition of partial riparian vegetation coverage, the measured C_r ($m^{1/2} \cdot s^{-1}$) values, hereinafter referred to as $C_{r, meas}$, have been calculated according to the following expression for Q_2 and Q_3 flow rates, in order to assess the experimental global water flow resistance:

$$C_{r, \, meas} = \frac{U}{\sqrt{R \cdot J}}, \tag{1}$$

where U ($m \cdot s^{-1}$) is the water flow average velocity, R (m) is the hydraulic radius, and J is the slope of the total energy line. The $C_{r,meas}$ values computed for the flow rates Q_2 and Q_3 without considering the DCM in combination with the four composite cross section methods [12–15] are respectively equal to 4.31 and 8.25 $m^{1/2} \cdot s^{-1}$.

2.7. Modeled Vegetative Chézy's Flow Resistance Coefficients: $C_{r,mod}$

2.7.1. Bp and S&S Resistance Predictor Models

The two global flow resistance predictor models examined in this study (Bp and S&S [8,9]) have been proposed for real riparian vegetation in emergent condition, i.e., when the water level (*h*) is smaller than the height of the stems measured from the vegetated reclamation channel bottom (h_v). Since the reed stems in the dormant phenological stage are characterized by a rigid biomechanical behavior [25], the two resistance predictor models have to be applied according to the following expressions:

Bp model resistance predictor model [8]:

$$C_r = \sqrt{\frac{1}{\frac{1}{C_b^2} + \frac{C_D \cdot a \cdot h}{2 \cdot g}}}, \tag{2}$$

where C_b ($m^{1/2} \cdot s^{-1}$) is the Chézy's coefficient flow resistance because of the bed roughness in vegetative emergent condition [26], and C_D is the stem's drag coefficient, equal to 1 for rigid cylindrical stems, as in our case. As indicated by Vargas-Luna et al. and Baptist [4,27], C_b can be calculated according to the following expression:

$$C_b = 18 \cdot log\left(\frac{12 \cdot h}{k_s}\right), \tag{3}$$

where k_s ($m^{1/2} \cdot s^{-1}$) is the characteristic bed roughness coefficient, equal to 50 $m^{1/2} \cdot s^{-1}$ for sand.

S&S resistance predictor model [9]:

$$C_r = 1.385 \cdot \left(1 - d \cdot \sqrt{m}\right) \cdot \sqrt{\frac{g}{a \cdot h}}, \tag{4}$$

where *d* (m) is the average stems' diameter, *m* (m^{-2}) is the riparian vegetation density (number of stems per unit channel bed surface), $a = m \cdot d$ (m) is the so-called projected riparian plant area per volume [4,27] and *g* ($m \cdot s^{-2}$) is the gravity acceleration.

2.7.2. *DCM* and Composite Cross Section Methods

In the present study, four composite cross section methods have been employed for characterizing the effect of the non-uniform vegetation distribution along the wetted perimeter on the global flow

resistance: Colebatch [12], Horton [13], Pavlovskii [14], and Yen [15]. These methods consider different weights for parametrizing the contribution of the three distinct DCM sub-sections on C_r, according to the following expressions:

Colebatch's composite cross section method [12]:

$$C_r = \left(\frac{\sum_{i=1}^{N} \sigma_i \cdot C_{ri}^{1.5}}{\sigma} \right)^{\frac{2}{3}} \tag{5}$$

Horton's composite cross section method [13]:

$$C_r = \left(\frac{\sum_{i=1}^{N} \chi_i \cdot C_{ri}^{1.5}}{\chi} \right)^{\frac{2}{3}} \tag{6}$$

Pavlovskii's composite cross section method [14]:

$$C_r = \left(\frac{\sum_{i=1}^{N} \chi_i \cdot C_{ri}^{2}}{\chi} \right)^{\frac{1}{2}} \tag{7}$$

Yen's composite cross section method [15]:

$$C_r = \frac{\sum_{i=1}^{N} \frac{\chi_i \cdot C_{ri}}{R_i^{\frac{1}{6}}}}{\frac{\chi}{R^{\frac{1}{6}}}} \tag{8}$$

where N is the number of the DCM sub-sections, while σ_i, χ_i, R_i, and C_{ri} respectively are the flow cross sectional area, the wetted perimeter, the hydraulic radius, and the vegetative Chézy's flow resistance coefficients calculated employing both *Bp* and *S&S* resistance predictor models [8,9] at each of the three DCM sub-sections (excluded DCM sub-section 2 in which the riparian vegetation was absent), while σ, χ, and R are the same parameters referred to the entire *ADV* cross section. The outcomes of these methods are hereinafter defined as $C_{r,mod}$.

2.8. Comparative Analysis between $C_{r,mod}$ and $C_{r,meas}$

The modeled vegetative Chézy's flow resistance coefficients, indicated as $C_{r,mod}$, have been compared with the experimental ones, indicated as $C_{r,meas}$, in order to evaluate their capability in predicting the experimental global flow resistance of vegetated channels for a condition of partial reed coverage at real scale.

We first compared $C_{r,meas}$ with the outcomes of Bp and S&S resistance predictor models [8,9], estimated without considering the actual cross sectional flow velocity distributions, and then, we carried out a second analysis comparing $C_{r,meas}$ with those obtained by combining *Bp and S&S* resistance predictor models [8,9] with the four cross section methods [12–15]. In both cases, the predictive efficiencies of the combination of the two examined resistance predictor models [8,9] have been assessed by computing the relative prediction error (ε_r, in %), for each of the two examined flow rates: Q_2 and Q_3, that can be expressed according to the following equation:

$$\varepsilon_r(\%) = \frac{C_{r,mod} - C_{r,meas}}{C_{r,meas}} \tag{9}$$

3. Results

3.1. Measured Vegetative Chézy's Flow Resistance Coefficients: $C_{r,meas}$

3.1.1. Field Morphometrical Vegetation Properties

The quantitative values of the field morphometrical vegetation properties recorded at the six measuring cross sections distributed along the reclamation channel are summarized in Table 1.

Table 1. Morphometrical vegetation properties measured at the six cross sections: *num.* is the number of stems in each measuring cross section, d (m) is the average stems' diameter, m (m^{-2}) is the riparian vegetation density and $\lambda = (\pi \cdot m \cdot d^2/4)$ is the riparian vegetation surface density.
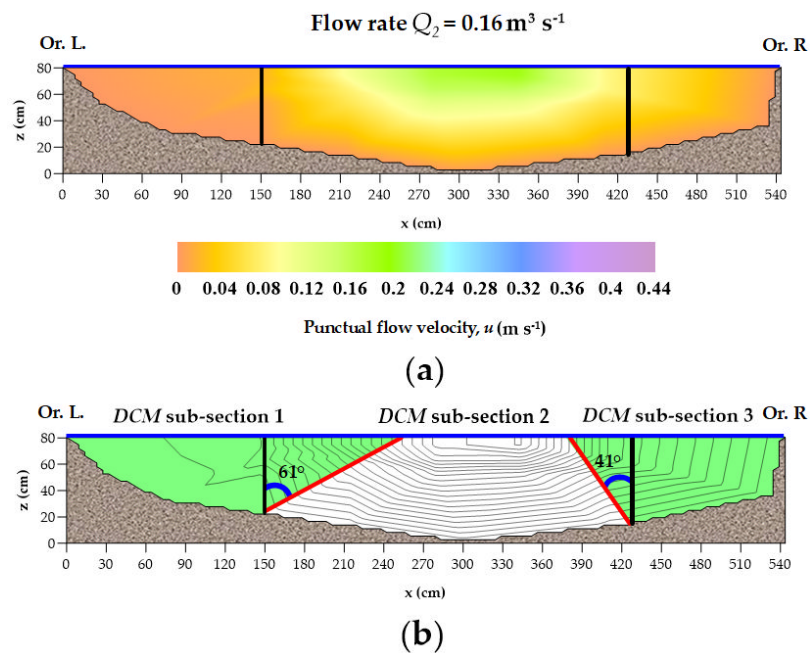
Cross Section	*num.*	d (m)	m (m^{-2})	λ	h_v (m)
1	270	0.0054	64	0.00146	2.50
2	165	0.0065	39	0.00130	2.30
3	159	0.0065	38	0.00126	2.23
4	198	0.0062	47	0.00142	2.10
5	182	0.0069	43	0.00161	2.35
6	245	0.0055	58	0.00138	2.50

In Table 1, *num.* is the total number of plants for each of the six cross sections and $\lambda = (\pi \cdot m \cdot d^2/4)$ is the so-called riparian vegetation surface density [4]. It is easy to observe that the cross sectional riparian vegetation distributions, synthetically expressed by λ, resulted to be very similar for all the six examined cross sections and thus it was assumed to be homogeneous along the entire reclamation channel, as already highlighted in Errico et al. [1]. Thus, also both experimental and modeled C_r retrieved at just the ADV cross section have been assumed to be representative of the conditions of the entire partly vegetated reclamation channel.
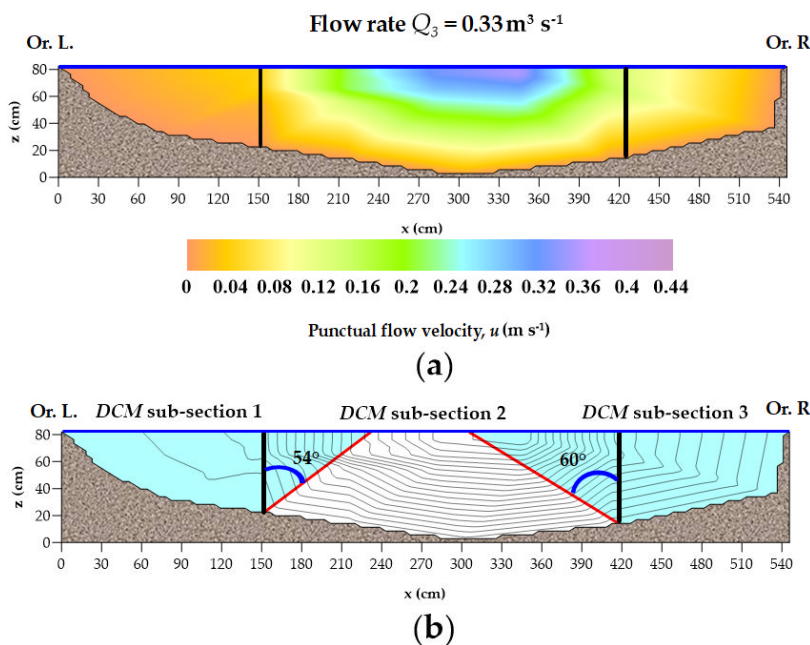
3.1.2. Cross Sectional Velocity Distributions

The experimental flow velocity distributions, also defined as isotachs, have been obtained by linearly interpolating the measured instantaneous flow velocities u (m·s^{-1}) acquired at the 15 points composing the ADV cross section measuring grid [1]. The experimental isotachs corresponding to the two examined flow rates Q_2 (= 0.16 m^3·s^{-1}) and Q_3 (= 0.33 m^3·s^{-1}) are respectively shown in Figures 7a and 8a. Three distinct sub-sections have been then defined by applying DCM, after a detailed analysis of the experimental isotachs. As shown in Figures 7b and 8b, the boundaries of the three DCM sub-sections have been delineated by drawing lines orthogonal to the isotachs starting from the channel bottom. Then, the slopes of these lines have been easily determined by means of simple geometrical computations. These lines correspond to the physical interface between water flow and riparian vegetation. The momentum exchange is null through these lines.

The side buffers of undisturbed riparian vegetation notably influenced the cross sectional flow velocity distribution for both Q_2 and Q_3 flow rate regimes, concentrating the water flow in the central region, cleared from vegetation, as depicted in Figures 7a and 8a. This phenomenon generates strong flow velocity gradients at the physical interface between the riparian vegetation buffers and the water flow [1] (continuous vertical black lines in Figures 7b and 8b) and affects significantly the slope of the boundary lines of the three DCM sub-sections: DCM sub-section 1, DCM sub-section 2 and DCM sub-section 3 (continuous vertical red lines in Figures 7b and 8b).

Figure 7. (**a**) Flow velocity field u (m·s^{-1}) for the Q_2 (= 0.16 m^3·s^{-1}) flow rate regime; (**b**) divided channel method (DCM) sub-sections. The continuous dark blue line indicates the water level at bankfull. The continuous vertical black lines indicate the boundary of the side buffers of undisturbed riparian vegetation, while the red lines represent the borders of the DCM sub-sections, in which slopes were equal to 61° and 41°, respectively referred to DCM sub-section 1 and DCM sub-section 3 (light green regions in Figure 7b). (From Lama et al. [3], modified).

Figure 8. (**a**) Flow velocity field u (m·s^{-1}) for the Q_3 (= 0.33 m^3·s^{-1}) flow rate regime; (**b**) DCM sub-sections. The continuous dark blue line indicates the water level at bankfull. The continuous vertical black lines indicate the boundary of the side buffers of undisturbed riparian vegetation, while the red lines represent the borders of the DCM sub-sections, in which slopes were equal to 54° and 60°, respectively referred to DCM sub-section 1 and DCM sub-section 3 (light blue regions in Figure 8b).

The Q_2 and Q_3 flow rate regimes were characterized by a turbulent water flow regime, since the Reynolds numbers Re (= $U \cdot h / \nu$, where U (m·s^{-1}) is the average flow velocity, h (m) is the water level

at bankfull, and ν (m$^2\cdot$s^{-1}) is the kinematic viscosity of water, equal to approximately 10^{-6} m$^2\cdot$s^{-1}) referred to these flow rates were respectively equal to 4.1×10^4 and 8.3×10^4. These values refer to the original values of hydraulic radius R, but they can be considered acceptable also for the condition of partial riparian vegetation cover, since the new values of R, referred to DCM sub-section 2 in which the flow motion was essentially concentrated, are similar to the original ones.

3.1.3. Bp and S&S Combined with Composite Cross Section Methods

The input parameters of the formulas of the four composite cross section methods examined in the present study [12–15], for each of the three DCM sub-sections described in the previous Section 3.1.2, are summarized in the following Tables 2 and 3, respectively referred to the two analyzed flow rates: Q_2 and Q_3. More in detail, χ_i and σ_i have been derived by considering separately the three DCM sub-sections delimited by the red borders indicated in Figures 7b and 8b, while h_i are the water levels at bankfull, measured from the bottom of each DCM sub-section, and m_i are the numbers of recorder stems per unit area, based on the survey plots 1 m × 1 m employed for the vegetation survey [1] falling into each DCM sub-section.

Table 2. Hydraulic and vegetative parameters referred to the flow rate $Q_2 = 0.16$ m$^3\cdot$s^{-1}: χ_i (m), σ_i (m^2), h_i (m) and m_i (m^{-2}) are respectively the wetted perimeter, the flow cross sectional area, the water level at bankfull and the riparian vegetation density of each *DCM* sub-section.

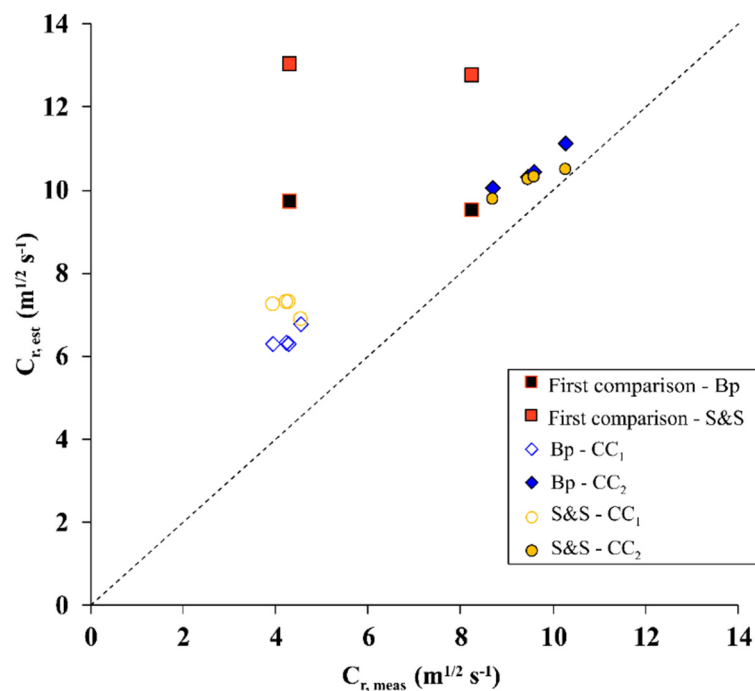| DCM Sub-Section	χ_i (m)	σ_i (m^{-2})	h_i (m)	m_i (m^{-2})
1	1.71	0.97	0.68	49
2	2.77	1.46	0.71	-
3	1.52	0.80	0.65	78

Table 3. Hydraulic and vegetative parameters referred to the flow rate $Q_3 = 0.33$ m$^3\cdot$s^{-1}: χ_i (m), σ_i (m^2), h_i (m) and m_i (m^{-2}) are respectively the wetted perimeter, the flow cross sectional area, the water level at bankfull and the riparian vegetation density of each *DCM* sub-section.

DCM Sub-Section	χ_i (m)	σ_i (m^{-2})	h_i (m)	m_i (m^{-2})
1	1.88	1.04	0.72	49
2	2.82	1.21	0.77	-
3	1.82	0.96	0.68	78

The riparian vegetation density m_i at DCM sub-section 2, corresponding to the central region of the entire examined reclamation channel, is null because the Common reed plants have been completely removed in that specific DCM sub-section [1].

3.1.4. Comparative Analysis between $C_{r,mod}$ and $C_{r,meas}$

A comparative analysis between $C_{r,mod}$ and $C_{r,meas}$ has been carried out in order to evaluate the predictive efficiency of the Bp and the S&S flow resistance predictor models [8,9] in the condition of partial vegetation cover of a reclamation channel. As shown in the following Figure 9, a first comparison has been executed between $C_{r,mod}$ and $C_{r,meas}$, the latter calculated without applying the composite section methods (indicated by filled orange and black squares). Then, by employing the methodology proposed in the present study to parametrize the effect of riparian vegetation on the actual cross sectional flow velocity distribution, a comparative analysis has been performed by applying the DCM [11] in combination with the four selected composite cross section methods: Colebatch [12], Horton [13], Pavlovskii [14], and Yen [15].
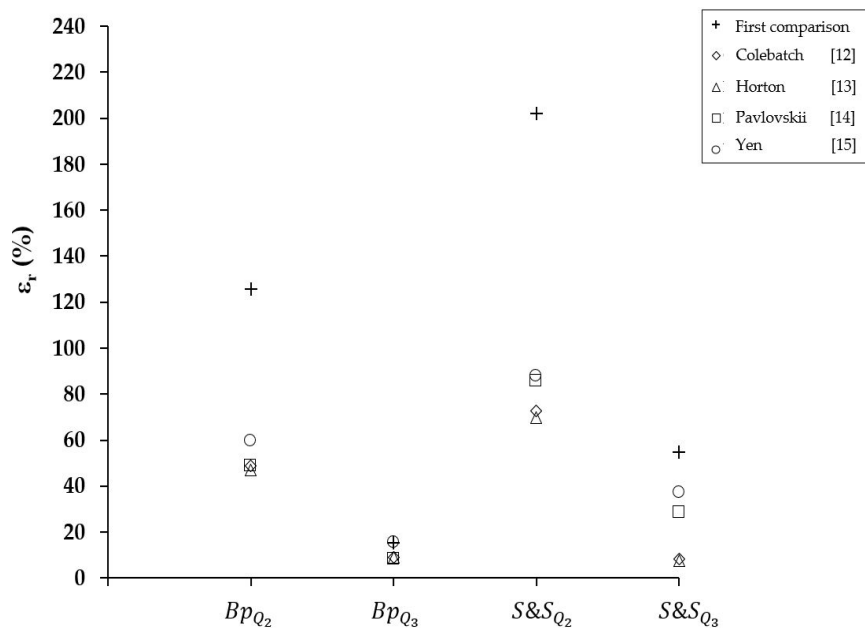
Figure 9. Measured and modeled C_r ($m^{1/2} \cdot s^{-1}$) for the Bp and S&S resistance predictors [8,9], by not applying (black and orange filled squares) and applying the four composite cross section methods: the blue diamonds and the yellow circles correspond respectively to Bp and S&S resistance predictor models, for $Q_2 = 0.16$ $m^3 \cdot s^{-1}$ (unfilled symbols) and $Q_3 = 0.33$ $m^3 \cdot s^{-1}$ (filled symbols). The dashed black line represents the perfect agreement between modeled and measured C_r.

Both Bp and S&S resistance predictor models [8,9] overestimated the measured C_r. The only remarkable difference between the two selected resistance predictor models is represented by the changing trend of the modeled C_r, depending on the two different investigated flow rates, as it can be noticed in Figure 9. In fact, for the Q_2 flow rate, Bp resistance predictor model [8] returned higher values than S&S [9], while this behavior was inverted when considering the Q_3 flow rate.

The relative prediction error ε_r (%) between $C_{r, mod}$ and $C_{r,meas}$ for the two examined resistance predictor models [8,9], for the Q_2 and Q_3 flow rates are shown in Figure 10. The combination of the two resistance predictor models examined in the present study [8,9] with the four composite cross section methods [12–15] for the two examined flow rates are respectively labeled as Bp_{Q_2}, Bp_{Q_3}, $S\&S_{Q_2}$, and $S\&S_{Q_3}$.

It can be easily observed that the Yen composite cross section method [15] systematically returned the highest ε_r value, for both Bp and S&S resistance predictor models [8,9] under both Q_2 and Q_3 flow rates. On the other hand, we can observe that in three cases Horton method [13] always returned the lower ε_r values, except for the case of S&S resistance predictor model [9] in combination with Pavlovskii method [14] under the Q_3 flow rate regime. In just one specific case, corresponding to Bp resistance predictor model [8] under the Q_3 flow rate regime, Yen composite cross section methods [15] returned $\varepsilon_r = 16\%$, close to that obtained by applying Bp and S&S resistance predictor models [8,9] without combining them with the four composite cross section methods, equal to 15%. For the Q_2 flow rate, ε_r reduced from 126% to 47% by combining Bp model [8] with Horton composite cross section method [13], and from 202% to 70% for S&S resistance predictor model [9] combined with the same method, while, for the Q_3 flow rate, ε_r decreased from 15% to 8% for Bp model [8] combined with Pavlovskii composite cross section method [14] and from 55% to 7% for S&S resistance predictor model [9] in combination with Horton composite cross section method [13]. Moreover, as it can be easily noticed, the highest reduction of ε_r with respect to the first comparison has been obtained by

combining Bp resistance predictor model [8] with Horton composite cross section method [13], for the Q_2 flow rate.

Figure 10. Relative prediction errors ε_r (%) of Bp and S&S resistance predictor models [8,9], computed under the two flow rate regimes respectively pair to $Q_2 = 0.16\,\text{m}^3 \cdot \text{s}^{-1}$ and $Q_3 = 0.33\,\text{m}^3 \cdot \text{s}^{-1}$, corresponding to the condition of partial riparian vegetation coverage of the reclamation channel, without employing the proposed methodology (black crosses), and by applying the four examined composite cross section methods: Colebatch [12] (diamonds), Horton [13] (triangles), Pavlovskii [14] (squares), and Yen [15] (circles).

4. Discussion

It is possible to notice from the analysis of the outcomes of the proposed methodology that the S&S resistance predictor model [9], in combination with Horton composite cross section method [13] exhibited the highest predictive performance, testified by the lowest ε_r, equal to 7%, achieved for the Q_3 flow rate. The Horton composite cross section method [13] assumes that the flow velocity is the same in the three DCM sub-sections; this assumption is not rigorously reliable for our study case, where it has been observed that DCM sub-section 2 carried most of the flow (Figures 7a and 8b). However, it led to reasonable results in terms of hydraulic roughness, comparable with those retrieved by employing the Colebatch method [14], because the wetted perimeters χ_i and the flow cross sectional area σ_i of each DCM sub-section are very similar, being the channel width of an order of magnitude lager than the water levels at bankfull.

Our results are in agreement with Yang et al. [28], who achieved a minimum prediction error (indicated in their work as relative accuracy) equal to 9.14%, computed by comparing the global flow resistances based on field measurements with those retrieved by employing a model based on unmanned aerial vehicles (UAV) techniques, in a river partially covered by emergent riparian vegetation. This is a promising finding since it demonstrates that the application of a simple methodology, like DCM [11] combined with one of the four examined composite cross section methods [12–15], can lead to results comparable with those obtained by using more complex models. The satisfactory levels of accuracy reached by the methodology proposed in the present study, testified by small ε_r values, have been achieved owing to the detailed analysis of the experimental ADV cross sectional flow velocity fields, that significantly affect the contributions of the different regions of the reclamation channel cross section to the global flow resistance for a condition of partial vegetation cover.

Moreover, the variability range of the ε_r values is very similar to that reported by Errico [29], which compared modeled and experimental roughness coefficients by applying different predictive models [30–32] in combination with the same composite cross section methods tested in the present study [12–15], but for a different scenario of partial vegetation coverage in a reclamation channel colonized by green and flexible Common reed plants. The main difference with respect to our outcomes is represented by the choice of the borders of the *DCM* sub-sections. In fact, Errico [29] considered just the vertical flow-vegetation physical interfaces, instead of those derived from the analysis of the experimental isotachs.

The evidences of the comparative analysis based on the proposed methodology can provide quantitative suggestions to administrators of land reclamation areas about the most appropriate methods for the parametrization of the field morphometrical vegetation properties that mostly affect the global flow resistance at real scale in partly vegetated reclamation channels [1,5], as a direct consequence of the hydrodynamic interaction between water flow and rigid Common reed plants in emergent conditions. In fact, the proposed methodology leads to a significant improvement in the accuracy of the examined resistance prediction models, with respect to those obtained without applying it. The presented findings are referred to the specific case of reclamation channels colonized by Common reed distributed along two lateral buffers at the sides. This aspect may constitute a limitation for the application on other riparian environments. However, we believe that in most vegetated channels the cross-sectional partitioning can represent a significant improvement of the global flow resistance estimation.

Further applications of the proposed methodology will be carried out on datasets obtained by remote sensing techniques from UAV, largely employed for measuring field morphometrical and bio-mechanical properties of vegetation in many agricultural, forestry, as well as in ecohydraulic studies referred to different vegetation species and phenological stages [29,33,34].

5. Conclusions

A direct comparative analysis between modeled and measured vegetative Chézy's coefficients C_r has been carried out, for assessing the predictive efficiencies of the Bp and the S&S resistance predictor models [8,9] for an experimental reclamation channel partly vegetated by rigid and emergent riparian Common reed plants, under two different flow rates. The accuracy of both resistance predictor models has been sensibly improved with respect to those obtained without applying the composite cross section methods [12–15]. These results have been achieved by applying a more rigorous physically based methodology, that considers the actual influence of the cross sectional riparian vegetation distribution on the flow velocity fields in conditions of partial reed cover. The proposed methodology, preliminarily introduced by Lama et al. [3], is founded on the analysis of the experimental isotachs retrieved from local ADV measurements at the upstream channel cross section [1]. We combined the Bp and S&S resistance predictor models [8,9] with DCM [12] and with four composite cross section methods: Colebatch [12], Horton [13], Pavlovskii [14], and Yen [15]. From the outcomes of the direct comparison between modelled and measured vegetative Chézy's coefficients C_r, it was observed that combination of the S&S resistance predictor model [8] and the Horton composite cross section method [13] returned the lowest value of relative prediction error ε_r, equal to 7%. The results of this study are limited to channels having a width of an order of magnitude lager than the water levels at bankfull.

From a computational fluid dynamics (CFD) perspective, the DCM constitutes a very simple model, based on basic theoretical assumptions. At the same time, it represents a quick method for describing the contribution of the distinct portions of the entire cross section characterized by the condition of partial riparian vegetation coverage. A significant improvement in the accuracy of the outcomes of the present study can be obtained by means of 2D and 3D numerical simulations, aiming at reproducing the actual impacts of the full and partial riparian vegetation coverage on the water flow velocity and turbulence cross sectional fields, by modelling the Common reed stems as rigid cylindrical

elements. Another improvement to this methodology can be achieved by analyzing the flow velocity vertical profile in detail, especially in correspondence of the interface between riparian vegetation buffers and water flow. In these cases, we can also consider the other methods (i.e., Kouwen et al. [35]) aiming at defining the influence of vegetation patches on global flow resistance.

It is possible to conclude that the outcomes of this study can provide to administrators of reclamation areas a simple and accurate methodology for modeling the real-scale effects of the cross sectional streamwise distributions on the global flow resistance of artificial and natural partly vegetated water bodies.

Notation

a	projected riparian plant area per volume
ADV	acoustic Doppler velocimeter
B	width of the ADV cross section
Bp	Baptist et al. (2007) resistance predictor model
Bp_{Q_2}	Baptist et al. (2007) resistance predictor model results for flow rate Q_2
Bp_{Q_3}	Baptist et al. (2007) resistance predictor model results for flow rate Q_3
C_b	Chézy's coefficient flow resistance due to the bed roughness
C_D	stem's drag coefficient
CFD	computational fluid dynamics
C_r	vegetative Chézy's flow resistance coefficient
$C_{r,\,meas}$	measured vegetative Chézy's flow resistance coefficient
$C_{r,\,meod}$	modeled vegetative Chézy's flow resistance coefficient
d	average stems' diameter
DCM	divided channel method
f''	vegetative Darcy-Weisbach's friction factor
g	gravity acceleration
h	water level at bankfull of the entire ADV cross section
h_i	water level at bankfull of each DCM sub-section
h_v	plants' height from the bottom of the vegetated reclamation channel
k_s	characteristic bed roughness coefficient, equal to 50 m$^{1/2}$ s^{-1} for sand
m	vegetation density of the entire ADV cross section
m_i	vegetation density of each DCM sub-section
N	number of the DCM sub-sections
n	Manning's hydraulic roughness coefficient
$num.$	number of stems recorded in each measuring cross section
Q_2	first examined flow rate, equal to 0.16 m^3 s^{-1}
Q_3	second examined flow rate, equal to 0.33 m^3 s^{-1}
R	hydraulic radius of the entire ADV cross section
R_i	hydraulic radius of each DCM sub-section
Re	Reynolds number
$S\&S$	Stone and Shen (2002) resistance predictor model
$S\&S_{Q_2}$	Stone and Shen (2002) resistance predictor model results for flow rate Q_2
$S\&S_{Q_3}$	Stone and Shen (2002) resistance predictor model results for flow rate Q_3
U	average flow velocity
u	instantaneous flow velocity
ε_r	relative prediction error
λ	riparian vegetation surface density
ν	kinematic viscosity of water, equal to approximately 10^{-6} m^2 s^{-1}
π	pi, equal to approximately 3.14
σ	flow cross sectional area of the entire ADV cross section
σ_i	flow cross sectional area of each DCM sub-section
χ	wetted perimeter of the entire ADV cross section
χ_i	wetted perimeter of each DCM sub-section

Conflicts of Interest: The authors declare no conflict of interest.

References

1. Errico, A.; Lama, G.F.C.; Francalanci, S.; Chirico, G.B.; Solari, L.; Preti, F. Flow dynamics and turbulence patterns in a reclamation channel colonized by Phragmites australis (common reed) under different scenarios of vegetation management. *Ecol. Eng.* **2019**, *133*, 39–52. [CrossRef]

2. Rowinski, P.M.; Västilä, K.; Aberle, J.; Järvelä, J.; Kalinovska, M.B. How vegetation can aid in coping with river management challenges: A brief review. *Ecohydrol. Hydrobiol.* **2018**, *8*, 345–354. [CrossRef]

3. Lama, G.F.C.; Errico, A.; Francalanci, S.; Chirico, G.B.; Solari, L.; Preti, F. Comparative analysis of modeled and measured vegetative Chézy's flow resistance coefficients in a reclamation channel vegetated by dormant riparian reed. In Proceedings of the International IEEE Workshop on Metrology for Agriculture and Forestry, Portici, Italy, 24–26 October 2019.

4. Vargas-Luna, A.; Crosato, A.; Uijttewaal, W.S.J. Effects of vegetation on flow and sediment transport: Comparative analyses and validation of predicting model. *Earth Surf. Proc. Land.* **2015**, *40*, 157–176. [CrossRef]

5. Errico, A.; Pasquino, V.; Maxwald, M.; Chirico, G.B.; Solari, L.; Preti, F. The effect of flexible vegetation on flow in reclamation channels. Estimation of roughness coefficients at real scale. *Ecol. Eng.* **2018**, *120*, 411–421. [CrossRef]

6. Västilä, K.; Järvelä, J. Modeling the flow resistance of woody vegetation using physically based properties of the foliage and stem. *Water Resour. Res.* **2014**, *50*, 229–245. [CrossRef]

7. Caroppi, G.; Västilä, K.; Järvelä, J.; Rowinski, P.M.; Giugni, M. Turbulence at water-vegetation interface in open channel flow: Experiments with natural-like plants. *Adv. Water Resour.* **2019**, *127*, 180–191. [CrossRef]

8. Baptist, M.J.; Babovic, V.; Rodríguez, J.; Keijzer, M.; Uittenbogaard, R.; Mynett, A.; Verwey, A. On inducing equations for vegetation resistance. *J. Hydraul. Res.* **2007**, *45*, 435–450. [CrossRef]

9. Stone, B.M.; Shen, H.T. Hydraulic resistance of flow in channels with cylindrical roughness. *J. Hydraul. Eng.* **2002**, *128*, 500–506. [CrossRef]

10. Errico, A.; Lama, G.F.C.; Francalanci, S.; Chirico, G.B.; Solari, L.; Preti, F. Validation of global flow resistance models in two experimental reclamation channels covered by *Phragmites australis* (common reed). In Proceedings of the 38th IAHR World Congress, Panama City, Panama, 1–6 September 2019.

11. Chow, V.T. *Open Channel Hydraulics*; McGraw-Hill: New York, NY, USA, 1959.

12. Colebatch, G.T. Model tests on the Lawrence Canal roughness coefficients. *J. Inst. Civil Eng. (Australia)* **1941**, *13*, 27–32.

13. Horton, R.E. Separate roughness coefficients for channel bottoms and sides. *Eng. News-Rec.* **1933**, *111*, 652–653.

14. Pavlovskii, N.N. On a design formula for uniform flow in channels with nonhomogeneous walls. *Trans. All-Union Sci. Res. Inst. Hydraulic Eng.* **1931**, *3*, 157–164. (In German)

15. Yen, B.C. Open channel flow resistance. *J. Hydraul. Eng.* **2002**, *128*, 20–39. [CrossRef]

16. Scotto di Perta, E.; Agizza, M.A.; Sorrentino, G.; Boccia, L.; Pindozzi, S. Study of aerodynamic performance of different wind tunnel configurations and air inlet velocities, using computational fluid dynamics (CFD). *Comput. Electron. Agr.* **2016**, *125*, 137–148. [CrossRef]

17. Caroppi, G.; Gualtieri, P.; Fontana, N.; Giugni, M. Vegetated channel flows: Turbulence anisotropy at flow–rigid canopy interface. *Geosciences* **2018**, *8*, 259. [CrossRef]

18.　Ozan, A.Y.; Yilmazer, D. Near-Wake Flow Structure of a Suspended Cylindrical Canopy Patch. *Water* **2019**, *12*, 84. [CrossRef]

19.　Goring, D.G.; Nikora, V.I. Despiking Acoustic Doppler Velocimeter Data. *J. Hydraul. Eng.* **2002**, *128*, 117–126. [CrossRef]

20.　King, A.T.; Tinoco, R.O.; Cowen, E.A. A k–ε turbulence model based on the scales of vertical shear and stem wakes valid for emergent and submerged vegetated. *J. Fluid Mech.* **2012**, *701*, 1–39. [CrossRef]

21.　Lama, G.F.C.; Errico, A.; Francalanci, S.; Chirico, G.B.; Solari, L.; Preti, F. Hydraulic modeling of field experiments in a reclamation channel under different riparian vegetation scenarios. In Proceedings of the AIIA Mid-Term Conference, Matera, Italy, 12–13 September 2019.

22.　Rhee, D.S.; Woo, H.; Kwon, B.; Ahn, H.K. Hydraulic resistance of some selected vegetation in open channel flows. *River Res. Appl.* **2008**, *24*, 673–687. [CrossRef]

23.　Faugno, S.; Quaquarelli, I.; Civitarese, V.; Crimaldi, M.; Sannino, M.; Ricciaridello, G.; Caracciolo, G.; Asirelli, A. Two-steps Arundo Donax L. harvesting in South Italy. *Chem. Eng. Trans.* **2017**, *58*, 265–270.

24.　Soana, E.; Bartoli, M.; Milardi, M.; Fano, E.A.; Castaldelli, G. An ounce of prevention is worth a pound of cure: Managing macrophytes for nitrate mitigation in irrigated agricultural watersheds. *Sci. Total Environ.* **2019**, *647*, 301–312. [CrossRef]

25.　Pasquino, V.; Saulino, L.; Pelosi, A.; Allevato, E.; Rita, A.; Todaro, L.; Saracino, A.; Chirico, G.B. Hydrodynamic behaviour of European black poplar (Populus nigra L.) under coppice management along Mediterranean river ecosystem. *River Res. Appl.* **2018**, *34*, 1–9. [CrossRef]

26.　van Velzen, E.; Jesse, P.; Cornelissen, P.; Coops, H. *Stroming-Sweerstand Vegetatie in Uiterwaarden; Handboek. Part 1 and 2*; Technical Report, RIZA Reports: Arnhem, The Netherland, 2003.

27.　Baptist, M.J. Modelling floodplain biogeomorphology. Ph.D. Thesis, Delft University of Technology, Delft, The Netherlands, 2005.

28.　Yang, S.; Wang, P.; Lou, H.; Wang, J.; Zhao, C.; Gong, T. Estimating River Discharges in Ungauged Catchments Using the Slope–Area Method and Unmanned Aerial Vehicle. *Water* **2019**, *11*, 2361. [CrossRef]

29.　Errico, A. The effect of flexible vegetation on flow in drainage channels. Field surveys and modelling for roughness coefficients estimation. Ph.D. Thesis, University of Florence, Florence, Italy, 2017.

30.　Nepf, H.M.; Vivoni, E.R. Flow structure in depth-limited, vegetated flow. *J. Geophys. Res.* **2000**, *105*, 28457–28557. [CrossRef]

31.　James, C.S.; Birkhead, A.L.; Jordanova, A.A.; O'Sullivan, J.J. Flow resistance of emergent vegetation. *J. Hydraul. Res.* **2004**, *42*, 390–398. [CrossRef]

32.　Yang, W.; Choi, S.-U. A two-layer approach for depth-limited open-channel flows with submerged vegetation. *J. Hydraul. Res.* **2010**, *48*, 466–475. [CrossRef]

33.　Sarghini, F.; De Vivo, A. Analysis of Preliminary Design Requirements of a Heavy Lift Multirotor Drone for Agricultural Use. *Chem. Eng. Trans.* **2017**, *58*, 635c620.

34.　Giannetti, F.; Chirici, G.; Gobakken, T.; Næsset, E.; Travaglini, D.; Puliti, S. A new approach with DTM-independent metrics for forest growing stock prediction using UAV photogrammetric data. *Remote Sens. Environ.* **2018**, *213*, 195–205. [CrossRef]

35.　Kouwen, N.; Unny, T.E.; Hill, H.M. Flow retardance in vegetated channels. *J. Irrig. Drain. Div.* **1969**, *95*, 329–342.